Supporting Information for

Nsp3-N interactions are critical for SARS-CoV-2 fitness and virulence

Pengfei Li[1], Biyun Xue[2], Nicholas J. Schnicker[3], Lok-Yin Roy Wong[1], David K. Meyerholz[4], Stanley Perlman[1,2]*

[1]Department of Microbiology and Immunology, University of Iowa, Iowa City, IA, USA.

[2]Department of Pediatrics, University of Iowa, Iowa City, IA, USA.

[3]Protein and Crystallography Facility, University of Iowa, Iowa City, IA, USA.

[4]Department of Pathology, University of Iowa, Iowa City, IA, USA.

Running title: NSP3 SARS-Unique Domain S676T mutation alters SARS-CoV-2 fitness.

* Corresponding author: Stanley Perlman, stanley-perlman@uiowa.edu

Key words: SARS-CoV-2, Nsp3, SARS-unique domain, N protein.

This PDF file includes:

Supplementary Materials and Methods

Supplementary figures S1-S7 (including legends)

Supplementary table S1-S2

SI References

SI Materials and Methods

Plasmids

pcDNA3.1-Paip1-Flag (OHu17446) was purchased from GenSmart™. cDNA encoding PAIP1 amplified from pCI-MS2V5-PABPC1 (Addgene plasmid # 65807) with a V5 tag was inserted into pCAGGS mammalian expression vector. The SUD cDNA with either a Myc or Flag tag was amplified from pBAC-SARS-CoV-2 and then cloned into a pCAGGS vector. cDNAs of nsp3 N-terminal part including UBL1, UBL1 to SUD, and of N, with added V5 and Flag tags, were amplified from pBAC-SARS-CoV-2 and cloned into with a pCAGGS vector. pRL-TK (Renilla luciferase) was purchased from Promege (Madison, WI, USA) and modified as follows. Briefly, fragments of SARS-CoV-2 5' UTR and human beta-globin (HBB) were amplified from pBAC-SARS-CoV-2 and pJP-HBB-nLuc (Addgene, plasmid #175431) respectively, and then subcloned to replace the original 5'UTR of pRL-TK Vector. SARS-CoV-2 3' UTR amplified from pBAC-SARS-CoV-2 was positioned downstream of the Renilla luciferase gene in the 5' UTR-containing reporter. Reporter plasmids containing the 5' leader, nsp3-S676T mutants and N-S194L mutants were generated using site-directed mutagenesis as previously described (1). Sequences of all constructs were verified prior to use. All primers are listed in *SI Appendix* Supplementary Table S1.

Generation of recombinant viruses

All the recombinant viruses in this study were generated based on pBAC-SARS-CoV-2 using lambda red recombination with I-SceI homing endonuclease as previously described (2, 3). Briefly, forward and reverse primers (*SI Appendix* Supplementary Table S1) containing overlapping sequences homologous to viral RNA with the desired mutations, flanked by sequences for amplifying a Kan^r-I-SceI fragment were designed and synthesized. PCR products were generated using these primers from pEP-Kan-I-SceI (4) and were electroporated into GS1783 E. coli cells containing pBAC-SARS-CoV-2. Clones containing the desired sequences were selected and treated with arabinose to produce I-SceI, which induced recombination to remove the Kan^r-I-SceI fragment. Desired clones were chloramphenicol-resistant and kanamycin-sensitive and were selected for further verification by sequencing. Vero-E6 cells were grown on 12-well plates to 60–80% confluency and then transfected with recombinant pBAC (1ug) using Lipofectamine 3000. When cytopathic effects (CPE) reached 70%, supernatants were centrifuged to remove cell debris and processed for propagation on Calu-3 2B4 cells. Recombinant viruses were titered on Vero-E6 cells by plaque assay.

Virus infection

All experiments with SARS-CoV-2 were carried out in a Biosafety Level 3 (BSL3) Laboratory at the University of Iowa. Mice were lightly anesthetized with ketamine/xylazine and intranasally inoculated with the indicated amounts of SARS-CoV-2 in DMEM (50 µL). Mouse was monitored daily to evaluate the weight and mortality. In all cases, mice that did not survive all succumbed to the infection or were sacrificed because they were moribund. No mice were euthanized because they reached a low body weight. Vero-E6/Calu-3 (3×10^5/well) or human MDMs (5×10^5/well) were seeded on 12 wells plates for 16h prior to infection. Viruses were inoculated onto cells at the indicated multiplicity of infection (MOI), and plates were gently rocked each 15 min. After 1h, cells were washed by PBS 3 times and cultured in DMEM with 2% FBS. At indicated times, viruses were collected from supernatants and titered by plaque assay. HAEs (5×10^5/well) were grown in transwells containing collagen-coated 0.4 µm pore PTFE membranes in 24 well plates. Viruses were inoculated onto the apical sides at 0.1 MOI. After 2h, the inoculum was discarded, and the infected HAEs were washed with PBS. The basal chamber was replaced with fresh culture media. At 24 and 48h post-infection, 200 µL PBS was added to the apical side of the HAEs and cells were incubated for 30 min at 37°C to collect the released viruses. Viruses were then titered. For virus infection of human macrophages, cells (2×10^5/well) grown in 24 wells plates were inoculated with 1 MOI of the indicated viruses. Cells were lysed with TRIzol and RNA was prepared for analysis of viral mRNA levels by qPCR. For virus infection in the context of eIF4G or eIF4E knockdown, Vero E6 grown in 12 wells plates were transfected with siRNA targeting eIF4G (sc-35286, Santa Cruz Biotechnology), eIF4E (sc-35284, Santa Cruz Biotechnology) or a negative control using Lipofectamine 3000 (Thermo Fisher Scientific). After 48 h, cells were inoculated with the indicated viruses at 0.05 MOI as described above. At 24 hpi, cells were processed for infectious virus titer and for quantification of viral RNA as described above.

Viral plaque assay

Viruses from cell or lung homogenates were serially diluted in DMEM. 200 µL of diluted viruses were inoculated onto Vero-E6 cells in 12 wells plates for 1h. Plates were gently rocked every 15 min. After discarding the inoculum, the infected cells were overlaid with 0.6% agarose containing 2% FBS. After 3 days, cells were fixed with 10% formaldehyde, and the plaques were counted after staining with 0.1% crystal violet.

Real-time quantitative PCR

Total RNA was extracted from cells lysates or mice lungs using TRIzol reagent (Invitrogen) according to the manufacturer's protocol. DNase-treated RNA (1µg) was subjected to reverse transcription and the resulting cDNA was used to quantify expression of the indicated mRNAs by RT-qPCR. Housekeeping genes GAPDH, and HPRT were used as internal controls to normalize gene expression from cells, and mice, respectively. Average values from duplicates of each gene were used to calculate the relative abundance of transcripts normalized to GAPDH or HPRT and presented as $2^{-\Delta Ct}$. qPCR primers are shown in *SI Appendix* Supplementary Table S2.

Viral genome sequencing

In brief, viruses were inactivated by TRIzol reagent (Invitrogen), and the viral RNA were extracted using the Direct-zol RNA MiniPrep kit (Zymo Research) according to the manufacturer's instructions. ARTIC Version 4 (v4) primers were used for SARS-CoV-2. Nanopore sequencing (Oxford Nanopore Technologies) was performed by the University of Iowa State Hygienic Laboratory.

Co-immunoprecipitation and Western blotting assays

HEK-293T cells grown in 10 cm dishes were transfected with the indicated plasmids. After 24 h, cells were lysed with NP40 Cell Lysis buffer containing a protease inhibitor cocktail (Thermo Fisher Scientific). Supernatants were collected and clarified by centrifugation. Cell lysates were treated with Pierce™ Anti-Flag Affinity Resin (Thermo Fisher Scientific) for 2 h at 4°C. Resins were washed 3 times and boiled in 1x Laemmli sample buffer. The immunoprecipitates were subjected to SDS-PAGE followed by Western Blotting as previously described (5). Briefly, proteins separated by SDS-PAGE were transferred to nitrocellulose transfer membranes (Pall Corporation, East Hills, NY). Membranes were blocked with 5% skimmed milk, incubated with the indicated antibodies and visualized using an Odyssey® DLx Infrared Imaging System (LI-COR Biosciences). Primary antibodies used for Western blotting included: anti-Flag rat mAb (Biolegend), anti-V5 and anti-myc mouse mAb (Biolegend), anti-β-actin mouse mAb (Santa Cruz Biotechnology), anti-SARS-CoV-2-N mouse mAb and anti-SARS-CoV-2-N rabbit mAb (Sino Biological), anti-eIF4G and eIF4E mouse mAb (Santa Cruz Biotechnology), anti-Puromycin mouse mAb (Kerafast). IRDye® 800CW goat anti-mouse and IRDye® 800CW goat anti-rabbit IgG secondary antibodies were purchased from LI-COR Biosciences and used as secondary antibodies.

Luciferase assay

HEK-293T cells ($5x10^4$/well) were seeded onto 24 well plates, and cells were transfected with the indicated reporter plasmids (0.1 µg) along with plasmids expressing WT or S676T mutated SUD (1 µg) or empty control vector (1 µg) using Lipofectamine 3000 (Thermo Fisher Scientific) for 24h. Cells were lysed using 1x passive lysis buffer (Promega), and luciferase activity was measured using a Renilla luciferase assay kit (Promega) according to the manufacturer's protocol.

Human macrophage isolation

Human peripheral blood samples from leukocyte reduction cones were obtained from anonymous (de-identified) volunteers that had consented to blood donation at the DeGowin Blood Center at the University of Iowa. Protocols and consent forms were approved by the University of Iowa's Institutional Review Board. To obtain monocytes, peripheral blood mononuclear cells (PBMCs) were isolated by density gradient centrifugation through Ficoll-Paque PLUS density gradient media (Cytiva) and cultured at a seeding density of 1×10^6 cells/mL in RP-10 media (RPMI-1640 medium (GIBCO) with 10% FBS and 2 mM L-glutamine) supplemented with 5 ng/mL macrophage colony-stimulating factor (eBioscience). After 4 days, the cells were washed by Hanks' balanced salt solution (Invitrogen) to remove nonadherent cells. Adherent cells were trypsinized, pelleted, and cultured for 10 days.

In silico structural modelling

Amino acids 413-743 of nsp3 from SARS-CoV-2 Wuhan-Hu1 (NC_045512.2) were selected to model the structure of SUD or S676T-SUD using AlphaFold2 in Colab (6). Template mode (pdb70) was chosen since there are multiple solved structures for SUD. Five ranked structures using Amber relaxation were generated for SUD or S676T-SUD. The quality metrics including multiple sequence alignment (MSA) coverage, predicted aligned error (PAE), and predicted local distance difference test (pLDDT) for each group were listed in *SI Appendix* Figure S7. For the predicted structure of SARS-CoV (NC_004718.3) SUD, the nsp3 amino acid residues 389-720 were modeled using AlphaFold2 in Colab as before. The top ranked model of SUD from SARS-CoV or SARS-CoV-2 were used in Figure 1*D*. The alignment in Figure 4*F* was done using the helix residues 662-673 which precede the linker region. Hydrogen bonding analysis (Fig. 4*G*) was performed by selecting linker residues 674-678 and 685 and using PyMOL to find polar contacts within the selection for both S676-SUD and T676-SUD. The donor-to-acceptor cut off distance for hydrogen bonds is 3.6 Å in PyMOL.

Histopathological analysis

Paraffin-embedded lung tissues were stained with hematoxylin and eosin (HE) stain. Slides were examined by a boarded pathologist experienced with the model and masked by using a grouped masking approach (2, 7). Edema distribution in the lung were ordinally scored by: 0, none; 1, <25%; 2, 26–50%; 3, 51–75%; and 4, >75% of tissue fields. High resolution images were taken using a BX53 microscope, DP73 digital camera, and Cell Sens Dimension software (Olympus).

Statistical analysis

Log-rank (Mantel–Cox) test, two-tailed unpaired t-test with Welch's correction, two-tailed Wilcoxon matched-pairs test, and one-way ANOVA test with Tukey's multiple comparisons test were used in this study as described in the Figure Legends. Data are presented as mean ± s.e.m. $P < 0.05$ was considered statistically significant. *$P < 0.05$, **$P < 0.01$, ***$P < 0.001$; NS, not significant.

Fig. S1.

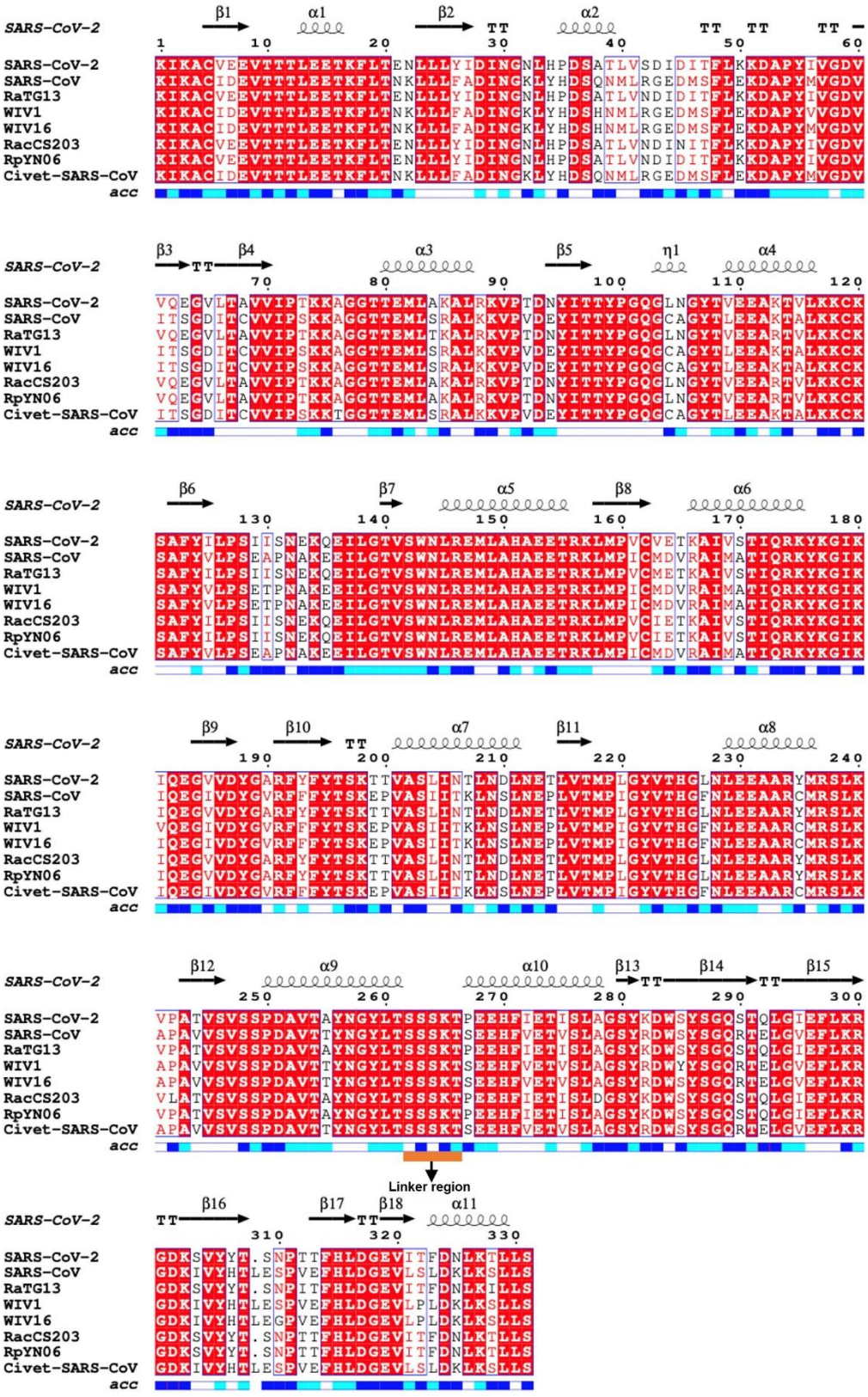
SARS-CoV-2
SARS-CoV
RaTG13
WIV1
WIV16
RacCS203
RpYN06
Civet-SARS-CoV
acc
Linker region

Fig. S1. Alignment of SUD amino acid sequences from different Sarbecoviruses.

The amino acid sequences of SUD from SARS-CoV-2 Wuhan-Hu-1 (NC_045512.2), SARS-CoV Tor2 (NC_004718.3), Bat coronavirus RaTG13(MN996532.2), Bat SARS-like coronavirus WIV1(KF367457.1), Bat SARS-like coronavirus WIV16 (KT444582.1), Bat coronavirus RacCS203 (MW251308.1), Betacoronavirus sp. RpYN06 strain bat/Yunnan/RpYN06/2020, and SARS coronavirus civet007 (AY572034.1) were downloaded from NCBI. The SUD sequence of SARS-CoV-2 with secondary structure information (built by AlphaFold2 in Colab) along with the SUD sequences from the other *Sarbecoviruses* was uploaded to ESPript 3.0 (8) to generate sequence alignment. Acc, accessibility. The amino acid numbers are based on the SARS-CoV-2 SUD.

Fig. S2.

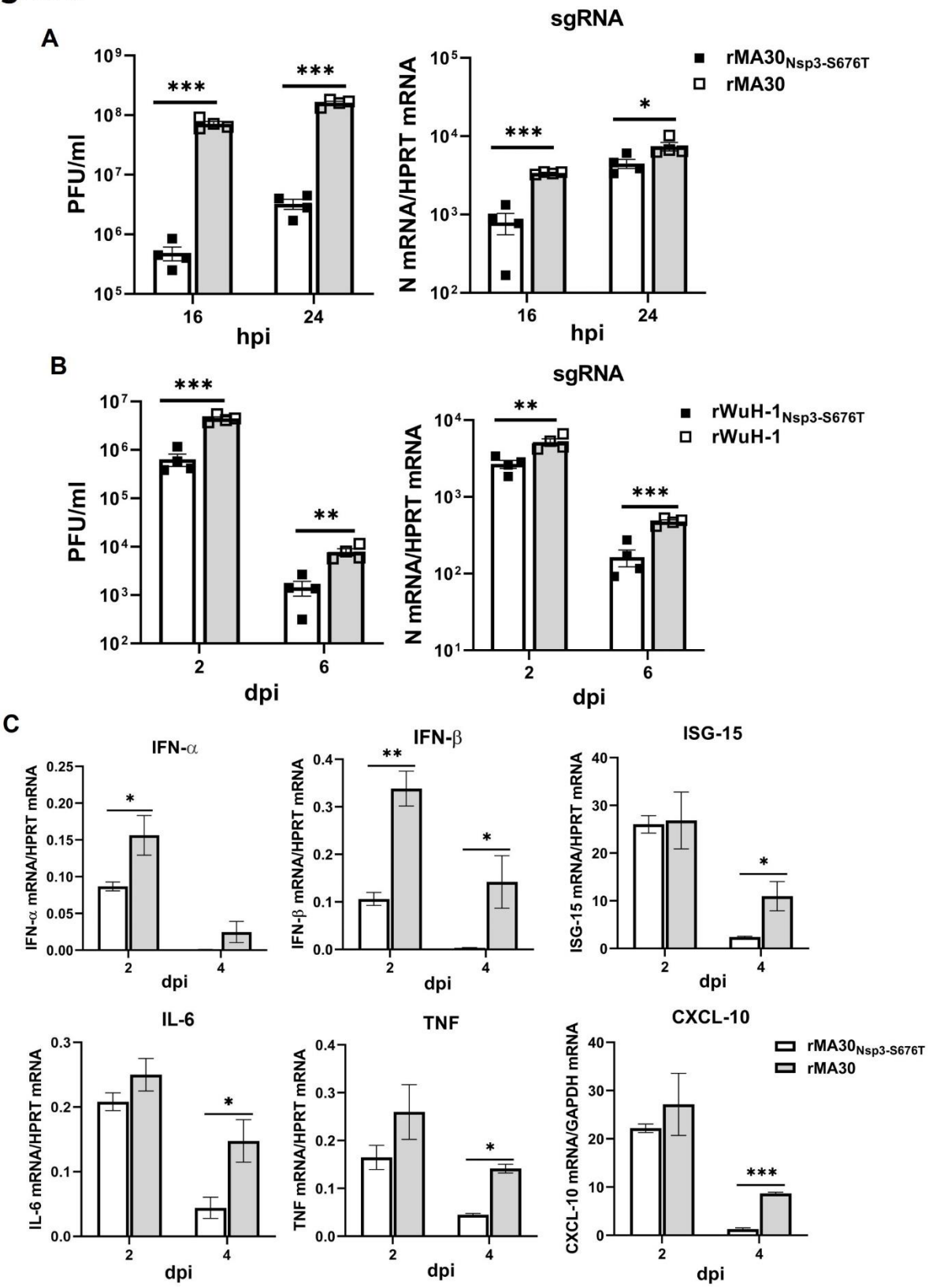
A
sgRNA
PFU/ml
N mRNA/HPRT mRNA
hpi
16
24
rMA30Nsp3-S676T
rMA30
B
sgRNA
PFU/ml
N mRNA/HPRT mRNA
dpi
2
6
rWuH-1Nsp3-S676T
rWuH-1
C
IFN-α
IFN-β
ISG-15
IL-6
TNF
CXCL-10
IFN-α mRNA/HPRT mRNA
IFN-β mRNA/HPRT mRNA
ISG-15 mRNA/HPRT mRNA
IL-6 mRNA/HPRT mRNA
TNF mRNA/HPRT mRNA
CXCL-10 mRNA/GAPDH mRNA
dpi
2
4
rMA30Nsp3-S676T
rMA30

179

Fig. S2. Cytokine expression in mice infected with virus containing NSP3 S676T.

(A) Lung virus titers and sgRNA levels in BALB/c mice infected with 5000 PFU of the indicated viruses at 16 and 24 hpi (n=4). (B) K18-hACE mice were inoculated with 2000 PFU of rWuH-1 or rWuH-$1_{Nsp3\text{-}S676T}$. At 2 and 6 dpi, lungs were harvested to measure viral titers and levels of sgRNA (n=4). (C) BALB/c mice were infected with 5000 PFU of rMA$30_{Nsp3\text{-}S676T}$ or rMA30, and total RNA from lungs at 2 and 4 dpi was subject to RT-qPCR to analyze expression of the indicated genes (n=3 mice, representative of two independent experiments). A two-tailed, unpaired t-test with Welch's correction was used to determine statistical significance.

Fig. S3.

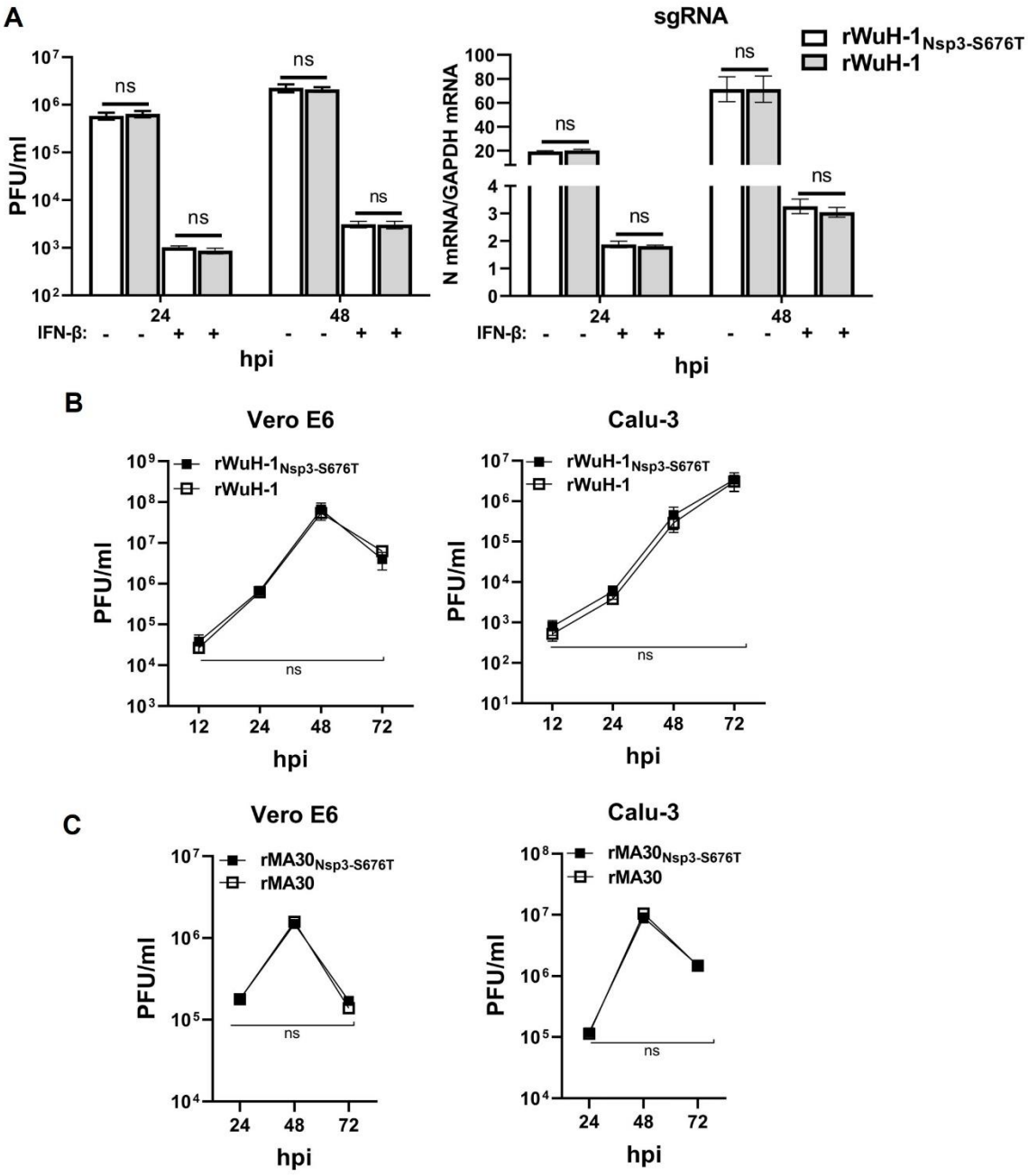

Fig. S3. Effect of IFN-β pre-treatment on virus replication and virus replication after infection at low MOI.

(A) Calu-3 cells pretreated with IFN-β (100 U) (PBL Assay Science) or PBS for 16 h were infected with rWuH-$1_{Nsp3\text{-}S676T}$ or rWuH-1 (0.05 MOI), At 24 and 48 dpi, supernatants and cell lysates were harvested for assessing virus titer and sgRNA levels, respectively. Representative of 2

independent experiments with 3 replicates/experiment. (B) Vero E6 and Calu-3 cells were infected with rWuH-1 or rWuH-$1_{Nsp3\text{-}S676T}$ at MOI=0.01. Supernatants were collected at 12, 24, 36 and 72 hpi to measure infectious viral titer by plaque assay (n=4 replicates, data combined from two experiments). (C) Vero E6 or Calu-3 cells were infected with 0.01 MOI of rMA30 or rMA$30_{Nsp3\text{-}S676T}$, and viral titers at 24, 36 and 72 hpi from supernatants were measured by plaque assay. Representative of 2 independent experiments with 4 replicates/experiment (B, C). Statistical significance was determined by a two-tailed, unpaired t-test with Welch's correction.

Fig. S4.

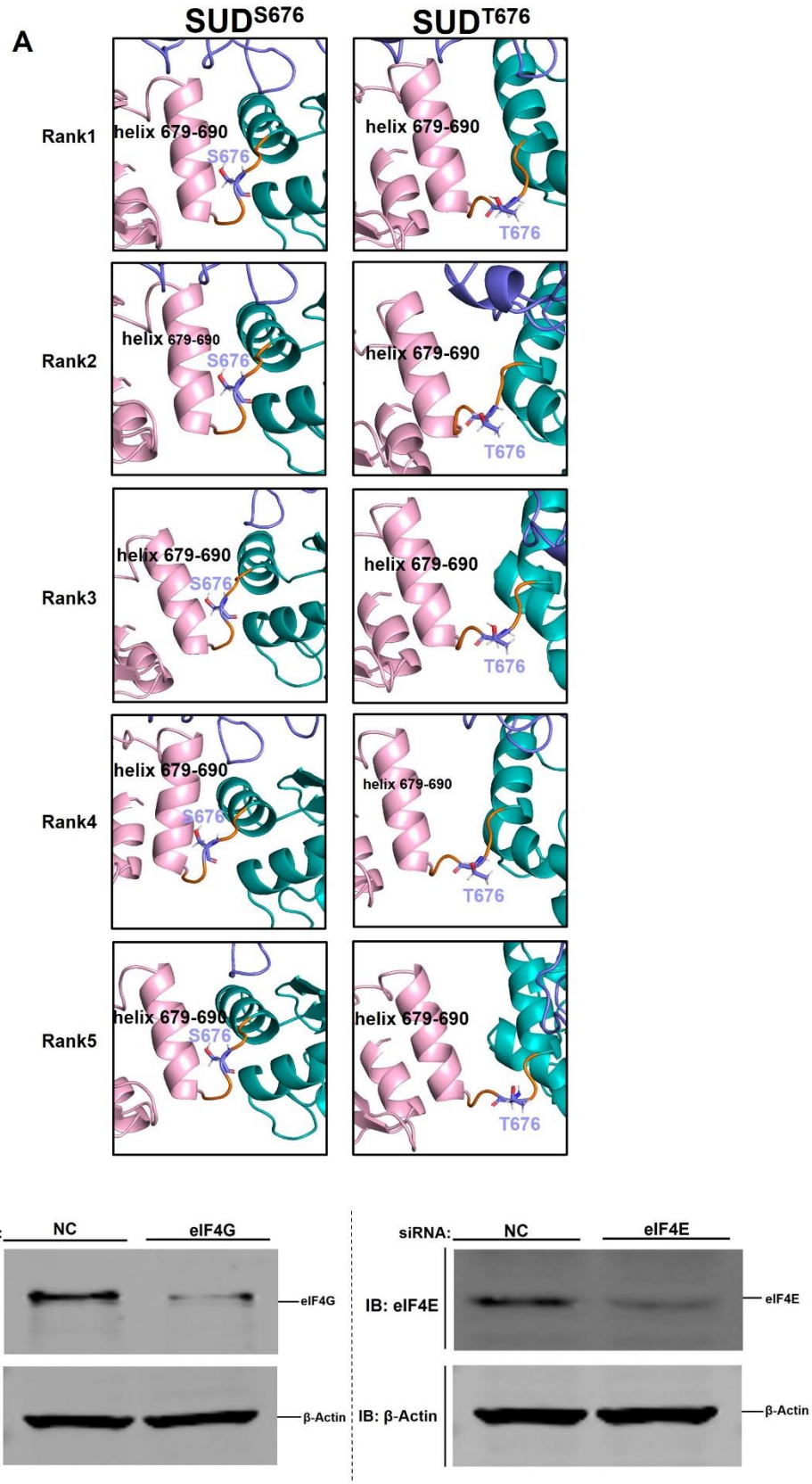
A
SUDS676
SUDT676
Rank1
Rank2
Rank3
Rank4
Rank5
helix 679-690
S676
T676
B
siRNA:
NC
eIF4G
eIF4E
IB: eIF4G
IB: eIF4E
IB: β-Actin
β-Actin

Fig. S4. AlphaFold2-based structures of nsp3-S676 and nsp3-T676.

(A) Top 5 ranked structures of the linker region of nsp3-S676 and nsp3-T676. All structures were built by AlphaFold2 in Colab as described in the Methods. Structures were further analyzed using PyMOL. Linker regions between SUD-M and SUD-C are colored in orange. Residues S676 and T676 are displayed by stick models. (B) Verification of eIF4G and eIF4E knockdown. Vero E6 cells were transfected with siRNAs targeting eIF4G or eIF4E at 40 nM. After 48h, cells were lysed in 1 x Laemmli buffer for Western blot analysis.

Fig. S5.

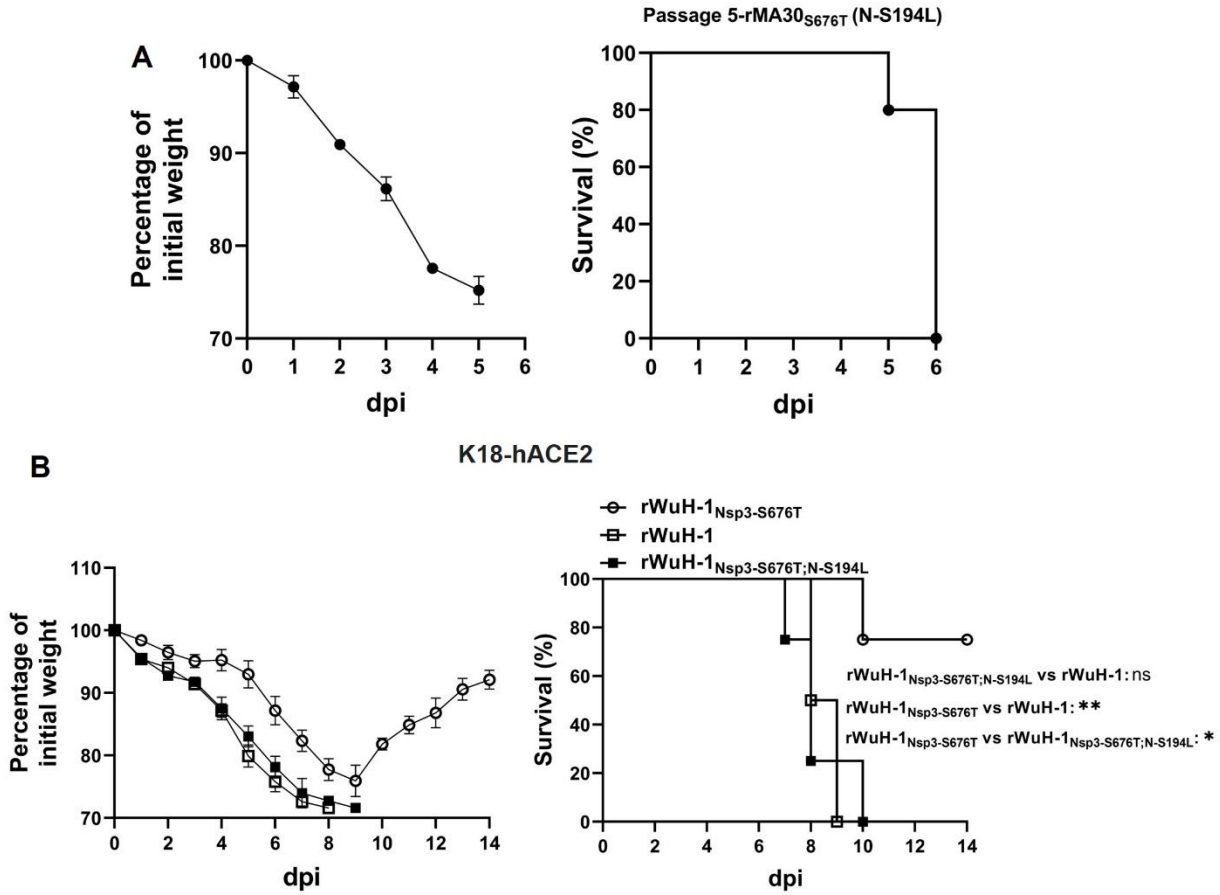

Fig. S5. Further characterization of N-S194L viruses. (A) Weight and survival of BALB/c mice infected with 5000 PFU of passage 5 mouse-adapted virus (#1 from Fig. 5*B*). (n=5) (B) K18-hACE2 mice infected with 2000 PFU of rWuH-1, rWuH-1$_{Nsp3\text{-}S676T}$ or WT$_{Nsp3\text{-}S676T;N\text{-}S194L}$ were monitored daily for weight changes and survival (n=4). Log-rank (Mantel–Cox) test were used to calculate *P* values.

Fig. S6.

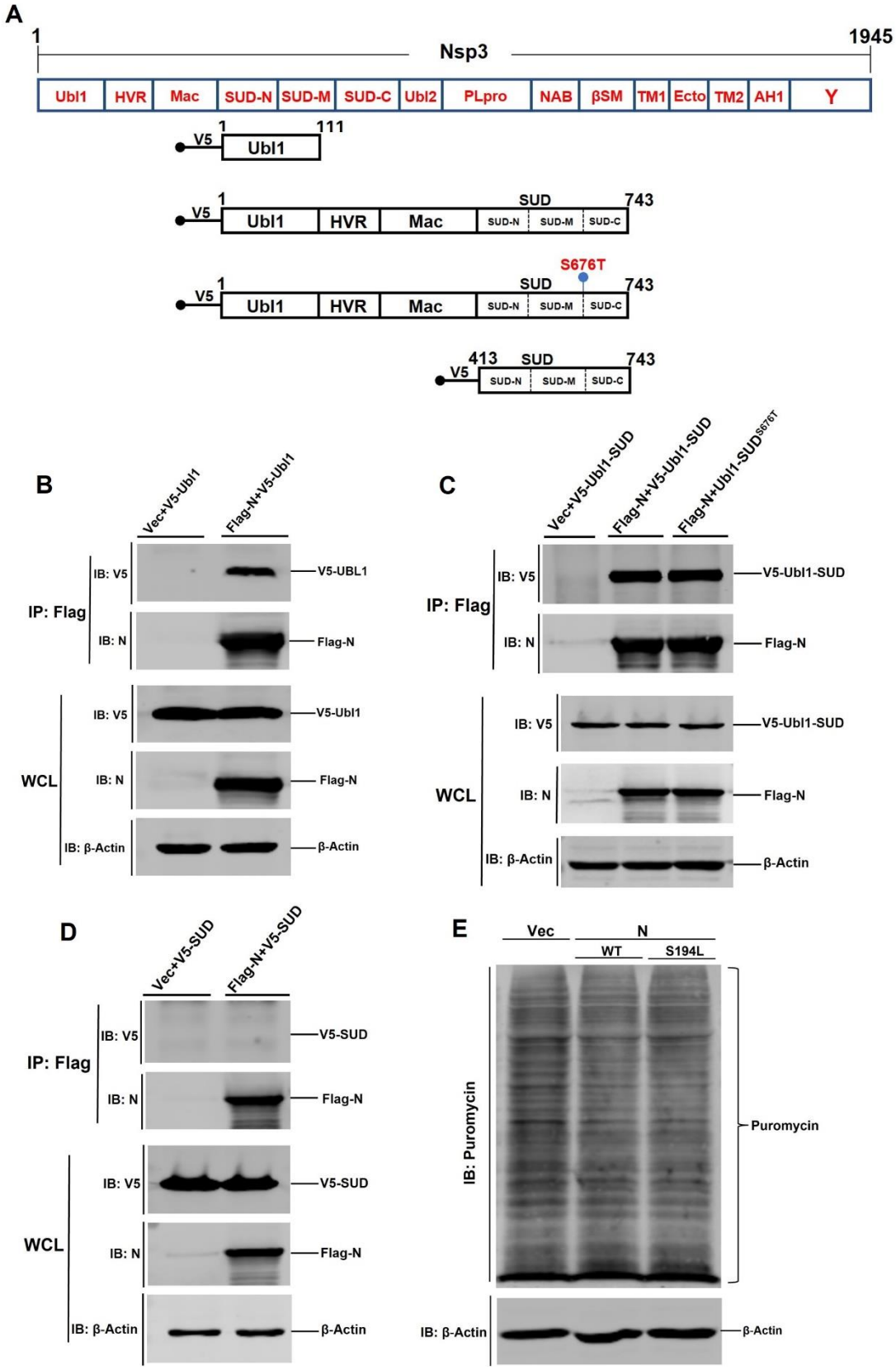
A
1
Nsp3
1945
Ubl1
HVR
Mac
SUD-N
SUD-M
SUD-C
Ubl2
PLpro
NAB
βSM
TM1
Ecto
TM2
AH1
Y
V5
111
SUD
743
S676T
413
B
Vec+V5-Ubl1
Flag-N+V5-Ubl1
IP: Flag
IB: V5
V5-UBL1
IB: N
Flag-N
WCL
V5-Ubl1
IB: β-Actin
β-Actin
C
Vec+V5-Ubl1-SUD
Flag-N+V5-Ubl1-SUD
Flag-N+Ubl1-SUD S676T
V5-Ubl1-SUD
D
Vec+V5-SUD
Flag-N+V5-SUD
V5-SUD
E
Vec
N
WT
S194L
IB: Puromycin
Puromycin

Fig. S6. The effect of S676T on the interaction of the N-terminal of Nsp3 and N. (A) Schematic of domain organization of nsp3 and N-terminal nsp3 truncated constructs. The numbers refer to the amino acid sequence of nsp3. Ubl, Ubiquitin-like domain. HVR, hypervariable region. Mac, macrodomain. PLpro, Papain-like protease domain. NAB, nucleic acid-binding domain. βSM, betacoronavirus-specific marker domain. TM, transmembrane domain. Ecto, ectodomain. AH1, amphipathic helix1. Y, unknown function. V5, V5-tag. (B-D) HEK-293T cells were transfected with V5-Ubl1, V5-Ubl1-SUD, V5-Ubl1-S676T-SUD or V5-SUD, individually with Flag-N. Co-transfection of vector and indicated truncated nsp3 constructs were controls. After 24h, cells were lysed. Lysates were immunoprecipitated with Pierce™ Anti-Flag Affinity Resin, and subjected to Western blotting analysis (Anti-SARS-CoV-2-N rabbit mAb was used for N protein staining). (E) Effects of N protein on cellular protein synthesis. HEK-293T cells were transfected with plasmids encoding Flag-N, Flag-N-S194L or vector. After 24 h, cells were incubated in medium containing 10 μg/mL puromycin for 30 min. Cell lysates were subject to western blotting with an anti-puromycin antibody. Data are representative of three independent experiments.

Fig. S7.

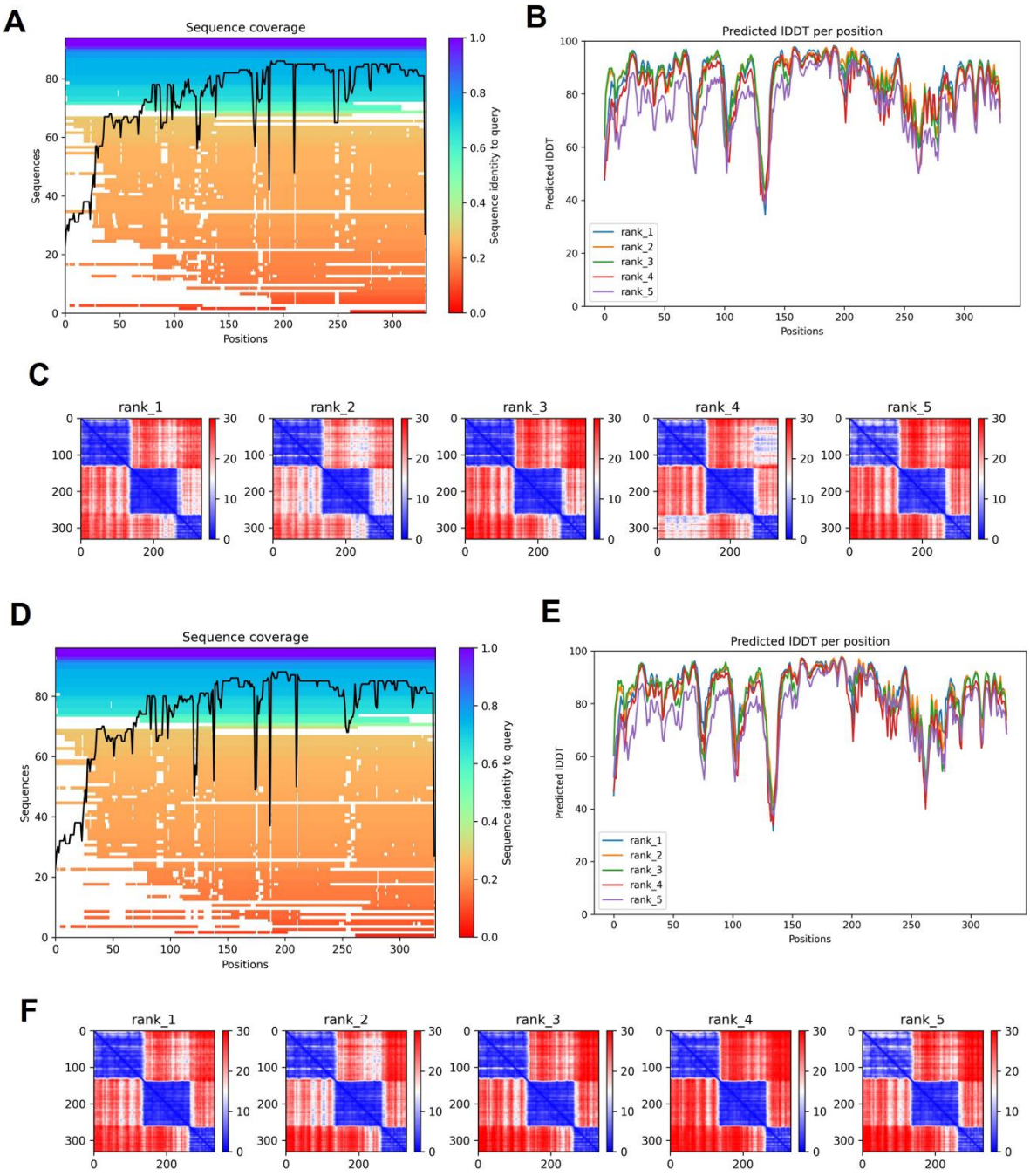
A
Sequence coverage
Sequences
Positions
Sequence identity to query
B
Predicted lDDT per position
Predicted lDDT
Positions
rank_1
rank_2
rank_3
rank_4
rank_5
C
rank_1
rank_2
rank_3
rank_4
rank_5
D
Sequence coverage
Sequences
Positions
Sequence identity to query
E
Predicted lDDT per position
Predicted lDDT
Positions
rank_1
rank_2
rank_3
rank_4
rank_5
F
rank_1
rank_2
rank_3
rank_4
rank_5

237

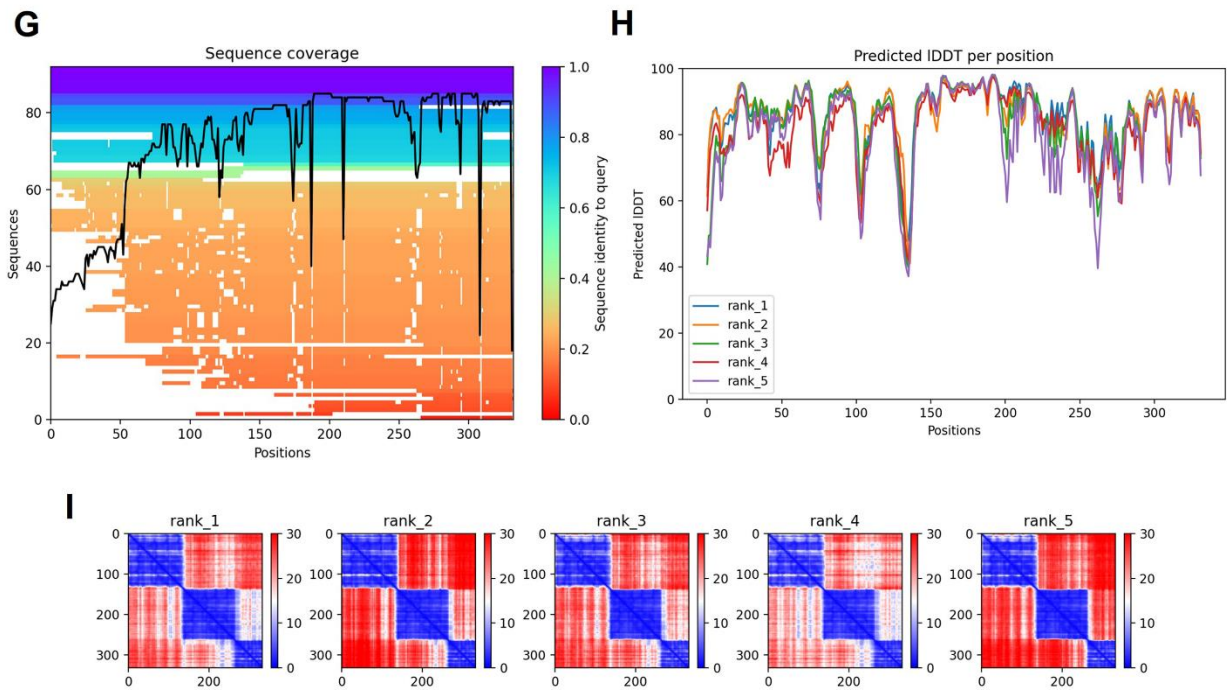

Fig. S7. MSA depth/diversity and confidence measures of SUD structure prediction

(A-C) MSA coverage (A), pLDDT (B) and PAE (C) for SARS-CoV-2 SUD^{S676} prediction fromAlphaFold2 in Colab. 5 top ranked predicted structures were generated.

(D-F) MSA coverage (D), pLDDT (E) and PAE (F) for SARS-CoV-2 SUD^{T676} prediction from AlphaFold2 in Colab. 5 top ranked predicted structures were generated.

(G-I) MSA coverage (G), pLDDT (H) and PAE (I) for SARS-CoV SUD as predicted by AlphaFold2 in Colab. 5 top ranked predicted structures were generated.

Supplementary Table S1. Primers for plasmid construction

Primer	5' → 3'
NSP3-S676T(T4547A)-Forward	GATGCTGTTACAGCGTATAATGGTTATCTTACTTCTTCTACTAAA ACACCTGAAGAACATAGGATGACGACGATAAGTAGGG
NSP3-S676T(T4547A)-Reverse	AGTGAGATGGTTTCAATAAAATGTTCTTCAGGTGTTTTAGTAGA AGAAGTAAGATAACCAGCCAGTGTTACAACCAATTAACC
N-S194L(C28854T)-Forward	AAGCCTCTTCTCGTTCCTCATCACGTAGTCGCAACAGTTTAAGA AATTCAACTCCAGGCAAGGATGACGACGATAAGTAGGG
N-S194L(C28854T)-Reverse	AGGAGAAGTTCCCCTACTGCTGCCTGGAGTTGAATTTCTTAAAC TGTTGCGACTACGTGAGCCAGTGTTACAACCAATTAACC
PABP1-Forward	CGGATCCACTAGTCCAGTGTGGTGGGCCACCATGGGCAAGCC CATCCCTAACCCACTGCT
PABP1-Reverse	GCTGATCAGCGGGTTTAAACGGGCCTTAAACAGTTGGAACACC GGTGGCACT
SUD-Forward	TCATTTTGGCAAAGAATTGCCACCATGAAAATCAAAGCTTGTGT TGAAGAAG
SUD-Reverse (*Myc-tag*)	TTTTGGCAGAGGGAAAAAGATCGAGCTCA*CAGATCCTCTTCTG AGATGAGTTTTTGTTC*AGAAAGAAGTGTCTTAAGATTGTCA
N-Forward	TCATTTTGGCAAAGAATTGCCACCATGTCTGATAATGGACCCCA AA
N-Reverse (*Flag-tag*)	TTTTGGCAGAGGGAAAAAGATCGAGTTA*CTTGTCGTCATCGTCT TTGTAGTC*GGCCTGAGTTGAGTCAGCACTGCT
Ubl1-SUD-Forward (*V5-tag*)	TCATTTTGGCAAAGAATTGCCACCATG*GGCAAGCCCATCCCTA ACCCACTGCTGGGCCTGGACAGCACC*GCACCAACAAAGGTTA CTTTTG
Ubl1-SUD-Reverse	TTTTGGCAGAGGGAAAAAGATCGAGTCAAGAAAGAAGTGTCTT AAGATTG
Ubl1-Reverse	TTTTGGCAGAGGGAAAAAGATCGAGTCACTCATCTGGAGGGTA GAAAGAA
SUD-Forward (*V5-tag*)	TCATTTTGGCAAAGAATTGCCACCATG*GGCAAGCCCATCCCTA ACCCACTGCTGGGCCTGGACAGCACC*AAAATCAAAGCTTGTGT TGAAG
SARS-CoV-2 5' UTR-Forward	AAGTTGGTCGTGAGGCACTGGGCAGATTAAAGGTTTATACCTT CCCAGGT
SARS-CoV-2 5' UTR-Reverse	CATAAACTTTCGAAGTCATGGTGGCCTTACCTTTCGGTCACACC CGGACG
HBB 5' UTR-Reverse	GGTGTCTGTTTGAGGTTGCTAGTGAACACAGTTGTGTCAGAAG CAAATGTCTGCCCAGTGCCTCACGACCAACTT
HBB 5' UTR-Forward/ (pRL-TK-Forward for assembling with SARS-CoV-2 5' UTR)	GCCACCATGACTTCGAAAGTTTATG
pRL-TK-Reverse for assembling with SARS-CoV-2 5' UTR constructs	CTGCCCAGTGCCTCACGACCAACTT
SARS-CoV-2 5' Leader-Forward	GCCACCATGACTTCGAAAGTTTATG
SARS-CoV-2 5' Leader-Reverse	GTTCGTTTAGAGAACAGATCTACAAGAG
SARS-CoV-2 3' UTR-Forward	CGAGTTCTCAAAAATGAACAATAACAATCTTTAATCAGTGTGTAA CA

SARS-CoV-2 3’ UTR-Reverse	TGTATCTTATCATGTCTGCTCGAAGGTCATTCTCCTAAGAAGCTATTAA
pRL-TK (5’ UTR)-Forward for assembling with SARS-CoV-2 3’ UTR	CTTCGAGCAGACATGATAAGATACA
pRL-TK (5’ UTR)-Reverse for assembling with SARS-CoV-2 3’ UTR	TTATTGTTCATTTTTGAGAACTCG

249

250

Supplementary Table S2. Primers for RT-qPCR

Primers	5' → 3'
SARS-CoV-2 N-Forward	GACCCCAAAATCAGCGAAAT
SARS-CoV-2 N-Reverse	TCTGGTTACTGCCAGTTGAATCTG
SARS-CoV-2 ORF1(Nsp12)-Forward	CCCTGTGGGTTTTACACTTAA
SARS-CoV-2 ORF1(Nsp12)-Reverse	ACGATTGTGCATCAGCTGA
Human GAPDH-Forward	GGAGCGAGATCCCTCCAAAAT
Human GAPDH-Reverse	GGCTGTTGTCATACTTCTCATGG
Mouse IFN-α-Forward	TCCATCAGCAGCTCAATGAC
Mouse IFN-α-Reverse	AGGAAGAGAGGGCTCTCCAG
Mouse IFN-β-Forward	TCAGAATGAGTGGTGGTTGC
Mouse IFN-β-Reverse	GACCTTTCAAATGCAGTAGATTCA
Mouse ISG15-Forward	GGCCACAGCAACATCTATGA
Mouse ISG15-Reverse	CGCAAATGCTTGATCACTGT
Mouse TNF-Forward	GAACTGGCAGAAGAGGCACT
Mouse TNF-Reverse	AGGGTCTGGGCCATAGAACT
Mouse IL-6-Forward	GAGGATACCACTCCCAACAGACC
Mouse IL-6-Reverse	AAGTGCATCATCGTTGTTCATACA
Mouse CXCL-10-Forward	GCCGTCATTTTCTGCCTCAT
Mouse CXCL-10-Reverse	GCTTCCCTATGGCCCTCATT
Mouse HPRT-Forward	GCGTCGTGATTAGCGATGATG
Mouse HPRT-Reverse	CTCGAGCAAGTCTTTCAGTCC

SI References

1. P. Li *et al.*, Dysregulation of the RIG-I-like Receptor Pathway Signaling by Peste des Petits Ruminants Virus Phosphoprotein. *J Immunol* **206**, 566-579 (2021).
2. L. R. Wong *et al.*, Eicosanoid signalling blockade protects middle-aged mice from severe COVID-19. *Nature* **605**, 146-151 (2022).

3. A. R. Fehr, Bacterial Artificial Chromosome-Based Lambda Red Recombination with the I-SceI Homing Endonuclease for Genetic Alteration of MERS-CoV. *Methods Mol Biol* **2099**, 53-68 (2020).
4. B. K. Tischer, J. von Einem, B. Kaufer, N. Osterrieder, Two-step red-mediated recombination for versatile high-efficiency markerless DNA manipulation in Escherichia coli. *Biotechniques* **40**, 191-197 (2006).
5. P. Li *et al.*, The Nucleoprotein and Phosphoprotein of Peste des Petits Ruminants Virus Inhibit Interferons Signaling by Blocking the JAK-STAT Pathway. *Viruses* **11** (2019).
6. M. Mirdita *et al.*, ColabFold: making protein folding accessible to all. *Nat Methods* **19**, 679-682 (2022).
7. D. K. Meyerholz, A. P. Beck, Principles and approaches for reproducible scoring of tissue stains in research. *Lab Invest* **98**, 844-855 (2018).
8. X. Robert, P. Gouet, Deciphering key features in protein structures with the new ENDscript server. *Nucleic Acids Res* **42**, W320-324 (2014).